

Differential Gene Transcription of Extracellular Matrix Components in Response to In Vivo Corneal Crosslinking (CXL) in Rabbit Corneas

Sabine Kling^{1,2}, Arthur Hammer^{2,3}, Emilio A. Torres Netto^{1,4}, and Farhad Hafezi^{1,2,5,6}

¹ Laboratory of Ocular Cell Biology, Center of Applied Biotechnology and Molecular Medicine, University of Zurich, Switzerland

² Laboratory of Ocular Cell Biology, University of Geneva, Switzerland

³ Hoptial ophtalmique Jules-Gonin, Fondation Asile des aveugles, Lausanne, Switzerland

⁴ Department of Ophthalmology, Paulista School of Medicine, Federal University of Sao Paulo, Sao Paulo, Brazil

⁵ ELZA Institute AG, Dietikon/Zurich, Switzerland

⁶ University of Southern California, CA, USA

Correspondence: Sabine Kling, PhD, University of Zurich, Center for Applied Biotechnology and Molecular Medicine, Winterthurerstrasse 190, 8057 Zurich, Switzerland. e-mail: kling.sabine@gmail.com

Received: 20 July 2017

Accepted: 25 October 2017

Published: 12 December 2017

Keywords: corneal crosslinking; differential transcription; glycosylation; extracellular matrix; corneal biomechanics

Citation: Kling S, Hammer A, Torres Netto EA, Hafezi F. Differential gene transcription of extracellular matrix components in response to in vivo corneal crosslinking (CXL) in rabbit corneas. *Trans Vis Sci Tech.* 2017; 6(6):8. doi:10.1167/tvst.6.6.8
Copyright 2017 The Authors

Purpose: We studied changes in gene transcription after corneal crosslinking (CXL) in the rabbit cornea in vivo and identified potential molecular signaling pathways.

Methods: A total of 15 corneas of eight male New-Zealand-White rabbits were de-epithelialized and equally divided into five groups. Group 1 served as an untreated control. Groups 2 to 5 were soaked with 0.1% riboflavin for 20 minutes, which in Groups 3 to 5 was followed by UV-A irradiation at a fluence of 5.4 J/cm². Ultraviolet A (UVA) irradiation was delivered at 3 mW/cm² for 30 minutes (Group 3, standard CXL protocol), 9 mW/cm² for 10 minutes (Group 4, accelerated), and 18 mW/cm² for 5 minutes (Group 5, accelerated). At 1 week after treatment, corneal buttons were obtained; mRNA was extracted and subjected to cDNA sequencing (RNA-seq).

Results: A total of 297 differentially transcribed genes were identified after CXL treatment. CXL downregulated extracellular matrix components (collagen types 1A1, 1A2, 6A2, 11A1, keratocan, fibromodulin) and upregulated glycan biosynthesis and proteoglycan glycosylation (GALNT 3, 7, and 8, B3GALT2). Also, CXL activated pathways related to protein crosslinking (transglutaminase 2 and 6). In 9.1% of the significantly different genes, CXL at 3 mW/cm² (Group 1) induced a more distinct change in gene transcription than the accelerated CXL protocols, which induced a lower biomechanical stiffening effect.

Conclusions: Several target genes have been identified that might be related to the biomechanical stability and shape of the cornea. Stiffening-dependent differential gene transcription suggests the activation of mechano-sensitive pathways.

Translational Relevance: A better understanding of the molecular mechanisms behind CXL will permit an optimization and individualization of the clinical treatment protocol.

Introduction

Until recently, corneal ectasia could not be treated and typically required corneal transplantation, involving the risks of infection, protracted wound healing, and rejection. In 1997, Spoerl et al.¹ proposed a new technique to increase the biomechanical stiffness of the cornea: corneal crosslinking (CXL). The treatment involves de-epithelialization of the

cornea, soaking the corneal stroma with a chromophore (Vitamin B2, riboflavin), and ultraviolet A (UVA) irradiation with 3 mW/cm² for an additional 30 minutes. Multiple studies have shown that CXL successfully stops keratoconus² progression and also arrests postsurgical corneal ectasia.³ Since its introduction, a number of modifications of the original treatment protocol have been proposed, aiming at increasing its efficacy, shortening treatment duration,

and reducing the risk of postoperative complications. The most widely used modified treatment protocol is accelerated CXL,⁴ using a higher irradiance in combination with a shorter irradiation time. However, several studies showed a reduced treatment efficacy. In clinical settings, a shallower demarcation line^{5–7} and minor corneal flattening^{7,8} was reported with accelerated CXL compared to standard CXL; in experimental settings, a lower tensile elastic modulus^{9,10} and a lower dry-weight after enzymatic digestion¹¹ were found. Further modified treatment protocols include iontophoresis-assisted,¹² trans-epithelial,¹³ hypo-osmolar,¹⁴ pulsed,¹⁵ contact lens-assisted,¹⁶ and customized¹⁷ CXL. All modified protocols share limited success: the increase in corneal stiffness is lower compared to that of the standard CXL treatment. A reason why it is difficult to optimize CXL is that its working principle is poorly understood. Although most mechanical strengthening would be expected if bonds were formed between collagen lamellae, x-ray scattering experiments indicate that bonds are formed rather at the collagen fibril surface and in the protein network surrounding the collagen.¹⁸ Also, the corneal swelling capacity is reduced strongly after CXL,¹⁹ suggesting that proteoglycans and glycosaminoglycans are involved.^{20,21} Clinical trials currently are performed to address the question whether CXL has the potential for primary refractive corrections of myopia²² and hyperopia. A better understanding of the basic mechanisms behind CXL would allow better adaptation of the protocol for different therapies, but also to identify its limitations.

One might speculate that the arrest of keratocornus progression induced by CXL implies long-term and permanent changes on transcriptional, translational, and/or posttranslational levels. This hypothesis is supported by the fact that the increase in corneal stiffness after CXL lasts²³ potentially longer than the actual collagen turnover in the corneal tissue and that significant—sometimes even progressive—corneal flattening is observed after CXL treatment.²⁴ There are different mechanisms of how CXL may change gene transcription: the generation of large amounts of reactive oxygen species (ROS) may activate signaling pathways^{25,26} with the potential of reintroducing homeostasis. Another mechanism may involve mechanotransduction,^{27,28} which means the process of converting mechanical signals into biochemical responses. Mechanical signals may result from dynamically acting forces, but also from remodeling of the extracellular matrix (ECM),

leading to changes in cell adhesion and cell–cell contact that finally determine the mechanical interaction with the surrounding matrix.^{29,30} Different mechanisms of action have been identified for mechanotransduction: certain ion-channels open in response to increased tension in the plasma membrane (observed during osmotic changes), proteins can unfold domains upon tension that reveal cryptic-binding, and phosphorylation may increase upon stretching.²⁷ These immediate changes may activate signaling pathways and/or gene transcription within minutes to hours.^{27,30,31}

The purpose of this study was to analyze the corneal transcriptome before and after CXL treatment to identify differentially transcribed candidate genes that potentially affect corneal stiffness.

Methods

Eight New Zealand White rabbits (2.5 kg weight) were purchased from Charles River Laboratories (Saint-Germaine-Nuelles, France). All experiments were approved by the local ethical committee and adhered to the ARVO Statement for the Use of Animals in Ophthalmic and Visual Research.

CXL Treatment Protocol

Rabbits were anesthetized with a subcutaneous injection of ketamine (Ketalar; Pfizer AG, Zurich, Switzerland) and xylazine (Rompun 2%, 20 mg ml⁻¹; Bayer, Basel, Switzerland). A total of 15 eyes then were assigned to one of five treatment groups ($n = 3$ per group). The corneas of all groups were de-epithelialized. Group 1 served as untreated control. Groups 2 to 5 corneas additionally received 0.1% riboflavin instillation during 20 minutes, using a suction ring. Group 2 served as riboflavin control. Group 3 corneas subsequently were irradiated with 3 mW/cm² during 30 minutes, Group 4 corneas with 9 mW/cm² during 10 minutes, and Group 5 corneas with 18 mW/cm² during 5 minutes. Riboflavin was not renewed during UV irradiation. Three different irradiances were included to study the effect of different degrees of biomechanical stiffening.¹⁰ Directly after treatment, antibiotic ointment (Ofloxacin, Floxal 0.3%; Bausch & Lomb, Zug, Switzerland) was administered prophylactically onto the cornea and repeated twice daily (until epithelial closure on postoperative days 3–4) to avoid infections. In addition, buprenorphin (Temgesic) was administered

subcutaneously twice daily at 50 µg/kg until epithelial closure.

Sample Preparation

One week after CXL treatment the rabbits were sacrificed (intravenous 120 mg/kg, Pentothal; Ospedalia AG, Hünenberg, Switzerland) and the corneas obtained with a trephine (8 mm diameter). The corneal tissue was immersed in RLT lysis buffer + 1% β-mercaptoethanol and homogenized, first with scissors and then with a tissue disruptor (Qiagen GmbH, Hilden, Germany). Afterwards, samples were frozen in liquid nitrogen and stored at −80°C.

Then, mRNA of the entire cornea, including epithelial, keratocyte, and endothelial cells, was extracted using an RNeasy kit (Qiagen) according to the manufacturer's instructions. mRNA quantity and quality were assessed with a spectrophotometer (Qbit; Life Technologies, Carlsbad, CA, USA) and the Agilent 2100 bioanalyzer (Agilent Technologies, Santa Clara, CA, USA), respectively.

Differential Gene Transcription

Equal amounts of mRNA (300 ng) were reverse transcribed, then cDNA sequencing (RNAseq) was performed with the HighSeq 2500 system (Illumina, San Diego, CA, USA) using the TruSeq stranded mRNA protocol with 100 single-end reads. The sequencing quality was controlled with FastQC v.0.11.2 leading to a Phred quality score of >28 corresponding to a 1/1000 chance of errors. TopHat v2.0.13 software was used for mapping against the reference genome. The alignment percentage was not optimal (~65%), probably due to low sequencing quality of the rabbit genome. As a consequence, multiple-mapping reads were not considered in the counts. Here, counts corresponded to the total number of reads aligning to a genomic feature. Biological quality control and summarization were done with RSeQC v2.4 and PicardTools v1.92 software, respectively. Only genes with a count above 10 in at least three samples were included for further analysis. The normalization and differential transcription analysis was performed with the R/Bioconductor package edgeR v.3.10.5, for the genes annotated in the reference genome.

Statistical Analysis

Differentially transcribed genes were determined for each individual treatment group using a General

Linear Model (GLM), a negative binomial distribution and a quasi-likelihood test. Ten pairwise comparisons (edgeR, GLM, quasi-likelihood F test) of the experimental groups were analyzed (Table 1). Instead of correcting the *P* values of the differentially transcribed genes with the Bonferroni method for multiple testing error, a different approach was chosen selecting significant genes according to the response of the whole set of CXL and control conditions. For this purpose, a composite null hypothesis, H_0 , was created summarizing the five most important comparisons. The condition CXL at 18 mW/cm² was excluded in this selection process, as its treatment efficacy is smallest, as shown experimentally^{9–11} and clinically^{5–8} and, hence, its meaningfulness is lower than the other comparisons.

$$H_0 = H_{\text{virgin}=3\text{mW}} | H_{\text{virgin}=9\text{mW}} | H_{\text{ribo}=3\text{mW}} | H_{\text{ribo}=9\text{mW}} | \sim H_{\text{virgin}=ribo} \quad (1)$$

and hence:

$$H_1 = \sim H_0 \\ = \sim H_{\text{virgin}=3\text{mW}} \& \sim H_{\text{virgin}=9\text{mW}} \& \sim H_{\text{ribo}=3\text{mW}} \& \sim H_{\text{ribo}=9\text{mW}} \& H_{\text{virgin}=ribo} \quad (2)$$

where H_1 is the composite null hypothesis. $H_{x=y}$ represents an individual null hypothesis, that is there is no difference between *x* and *y*. $\sim H_{x=y}$ represent a rejected null hypothesis, that is there is a difference between *x* and *y*. Each comparison between CXL (at 3 or 9 mW/cm²) and control (virgin or riboflavin) is expected to be significant. In contrast, the comparison between the two control conditions is expected not to be significant. A given gene then will be considered significant, if H_1 is true. With a confidence interval of 95%, the probability for a false positive in one comparison is:

$$P_i = (P_{\text{virgin} \sim 3\text{mW}}) \cdot (P_{\text{virgin} \sim 9\text{mW}}) \cdot (P_{\text{ribo} \sim 3\text{mW}}) \cdot (P_{\text{ribo} \sim 9\text{mW}}) \cdot (P_{\text{ribo}=\text{virgin}}) \quad (3)$$

The probability of $P_{\text{ribo}=\text{virgin}}$ cannot be calculated exactly, as it is the power of the test. However, assuming that the power is 1, we have neglected this term resulting in $P_i \leq 0.05^4$. Applied to the entire set of *n* = 9335 analyzed genes, the probability of having at least one false-positive can be calculated:

$$P_{\text{cumulative}} = 1 - (1 - P_i)^n \leq 0.0567 \quad (4)$$

This *P* value, $P_{\text{cumulative}}$, is comparable to the standard significance level. An alternative correc-

Table 1. Differential Gene Transcription was Computed for a Total of 10 Comparisons Between Different Treatment and Control Groups

Comparison Between Groups	# Significant Genes, at 5% FDR + FC ≥ 2	# Downregulated, FC ≥ 2	# Upregulated, FC ≥ 2
Riboflavin vs. virgin	2	1	1
CXL 3 mW 30 min vs. virgin	504	201	303
CXL 9 mW 10 min vs. virgin	18	10	8
CXL 18 mW 5 min vs. virgin	4	0	4
CXL 3 mW 30 min vs. riboflavin	862	341	521
CXL 9 mW 10 min vs. riboflavin	36	19	17
CXL 18 mW 5 min vs. riboflavin	1	1	0
CXL 9 mW 10 min vs. CXL 3 mW 30 min	161	93	68
CXL 18 mW 5 min vs. CXL 3 mW 30 min	165	88	77
CXL 18 mW 5 min vs. CXL 9 mW 10 min	0	0	0

tion for multiple testing is the Bonferroni method, which, however, can be applied only to one group at a time. The above-described whole-data-set approach is superior, as it accounts for the reproduc-

cibility of the CXL effect before correcting for multiple testing. Figure 1 illustrates that with Bonferroni correction, lower statistical significance (19 significantly different genes) can be reached than

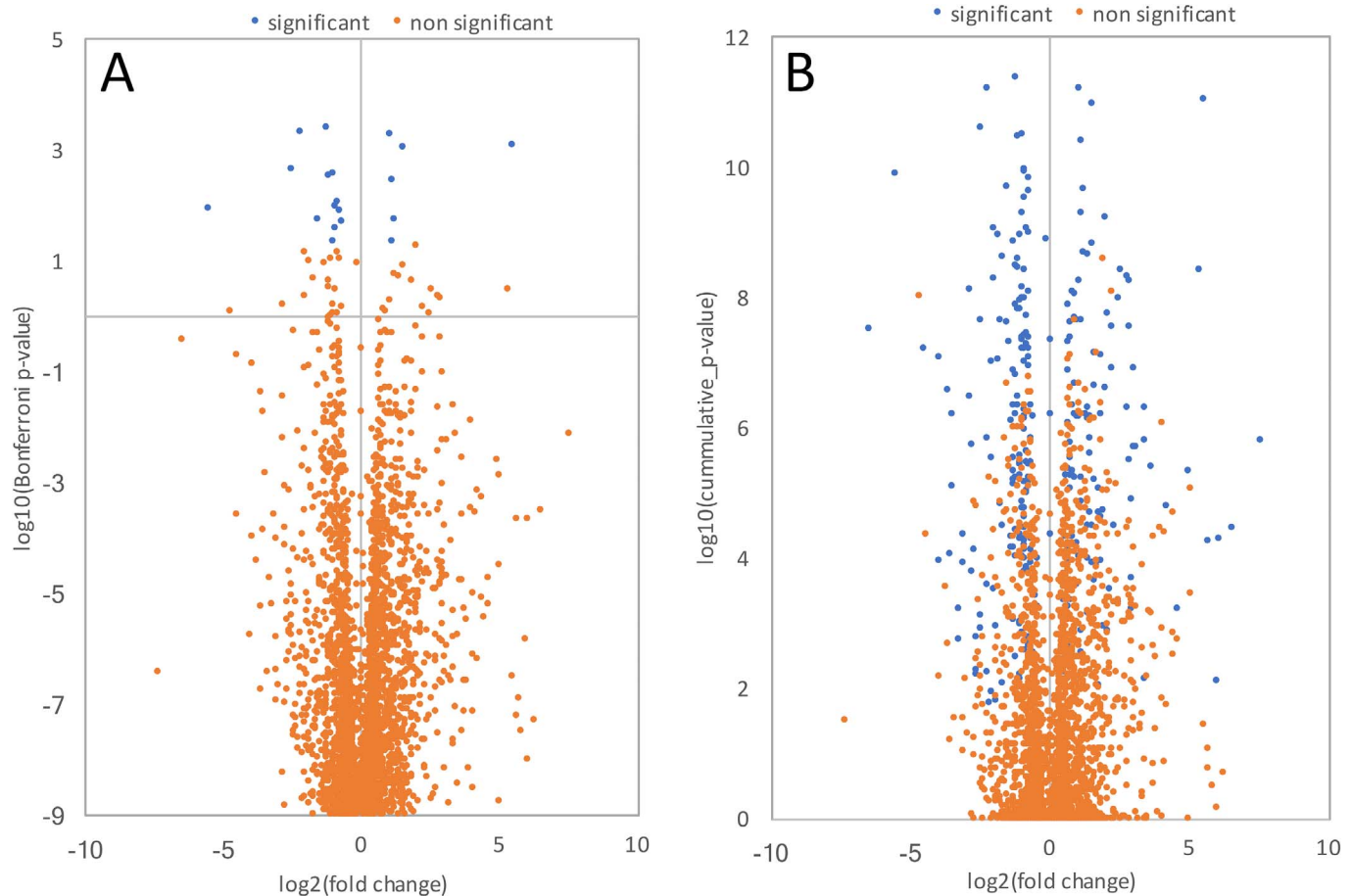


Figure 1. Comparison of different approaches to correct for multiple statistical testing. (A) Bonferroni method resulting in 19 significantly differently transcribed genes. (B) Whole-data-set method developed in this manuscript resulting in 297 significantly differently transcribed genes.

with the whole-data-set approach (297 significantly different genes).

Filter for Stiffening Dependent Gene Transcription

The resulting list of significantly transcribed genes then was subjected to filtering to determine genes that are transcribed differentially in a stiffening-dependent manner. The following criteria $\text{Filter}_{(\text{stiffening})}$ was imposed:

$$C_1 = [(\log\text{FC}_{\text{virgin}-3\text{mW}} > 0) \& (\log\text{FC}_{\text{virgin}-9\text{mW}} > 0) \\ \& (\log\text{FC}_{\text{virgin}-18\text{mW}} > 0) \& (\log\text{FC}_{\text{ribo}-3\text{mW}} > 0) \\ \& (\log\text{FC}_{\text{ribo}-9\text{mW}} > 0) \& (\log\text{FC}_{\text{ribo}-18\text{mW}} > 0) \\ \& (\log\text{FC}_{3\text{mW}-9\text{mW}} < 0) \& (\log\text{FC}_{3\text{mW}-18\text{mW}} < 0) \\ \& (\log\text{FC}_{9\text{mW}-18\text{mW}} < 0)] \quad (5a)$$

$$C_2 = [(\log\text{FC}_{\text{virgin}-3\text{mW}} < 0) \& (\log\text{FC}_{\text{virgin}-9\text{mW}} < 0) \\ \& (\log\text{FC}_{\text{virgin}-18\text{mW}} < 0) \& (\log\text{FC}_{\text{ribo}-3\text{mW}} < 0) \\ \& (\log\text{FC}_{\text{ribo}-9\text{mW}} < 0) \& (\log\text{FC}_{\text{ribo}-18\text{mW}} < 0) \\ \& (\log\text{FC}_{3\text{mW}-9\text{mW}} > 0) \& (\log\text{FC}_{3\text{mW}-18\text{mW}} > 0) \\ \& (\log\text{FC}_{9\text{mW}-18\text{mW}} > 0)] \quad (5b)$$

$$\text{Filter}_{(\text{stiffening})} = H_1 \& \sim H_{3\text{mW}=9\text{mW}} \& \sim H_{3\text{mW}=18\text{mW}} \\ \& (C_1 | C_2) \quad (5c)$$

where $\log\text{FC}$ is the fold-change in \log_2 scale between the different tested conditions; $\&$ and $|$ represent the logical operators AND and OR, respectively.

Correlation Analysis

The Pearson's linear correlation coefficient among all treatment conditions was calculated for selected differentially transcribed genes using Matlab software (Mathworks, Bern, Switzerland) to investigate mutual gene interactions. The online tool DAVID^{32,33} Bioinformatics Resources (Version 6.8) was used to extract related signaling pathways.

Results

Differential Gene Transcription

From a total of 9335 transcripts, 297 were significantly differentially transcribed between the two clinically efficient CXL conditions (at 3 and 9 mW/cm²) and controls (virgin and riboflavin). Of these differentially transcribed genes, 9.1% (27 genes)

were significantly stiffening-dependent, as per the definition above.

Most of the 297 differently transcribed genes were related to signaling (42), disulfide bonding (34), nucleotide binding (26), ATP binding (21), hydrolase (19), transferase (17), secreted (14), DNA binding (14), extracellular matrix (8), DNA replication (8), immunoglobulin domain (6), helicase (5), tyrosine protein kinase (5), collagen (3), DNA repair (3), and DNA damage (3). [Figure 2](#) presents a subset of pathways and genes that are likely involved in corneal mechanical properties.

Stiffening-dependent and -independent Differentially Transcribed Genes

[Table 2](#) and [Supplementary Table S1](#) present genes that were significantly differentially transcribed in a stiffening-dependent and stiffening-independent manner, respectively. Several genes of either subset have been reported previously to show an altered gene expression in keratoconus (references provided in the Tables).

[Figure 3](#) shows the change in normalized counts of selected genes for the different treatment and control conditions: Enzymatic crosslinking by transglutaminases 2 and 6 was increased significantly after CXL ([Figs. 3A, 3B](#)). Also, the expression of polypeptide N-acetylgalactosaminyltransferase 3 and β -1,3-galactosyltransferase 2, both related to the glycosylation of proteoglycans, was increased in crosslinked corneas ([Figs. 3C, 3D](#)). The only collagen type that was significantly upregulated after CXL was type IV, which forms part of the basement membrane. All other collagen types (I, VI, XI) were downregulated ([Figs. 3E–H](#)). Downregulation also was observed in noncollagenous ECM components, including thrombospondin 4 and keratocan ([Figs. 3I, 3J](#)). At the same time, enzymatic glycolysis by means of enolase 1 and transketolase was reduced in crosslinked corneas ([Figs. 3K, 3L](#)).

Most Affected Signaling Pathways after CXL Treatment

[Table 3](#) presents the two most affected pathways. Seven genes of the ECM receptor interaction pathway and 19 genes of the glycan biosynthesis and metabolism pathway were significantly differentially transcribed.

Correlation analysis

[Figure 4](#) shows genes that strongly correlated ($c_{\text{pearson}} > 0.8$, $P > 0.05$) with thrombospondin 4, a matricellular protein that is involved in tissue

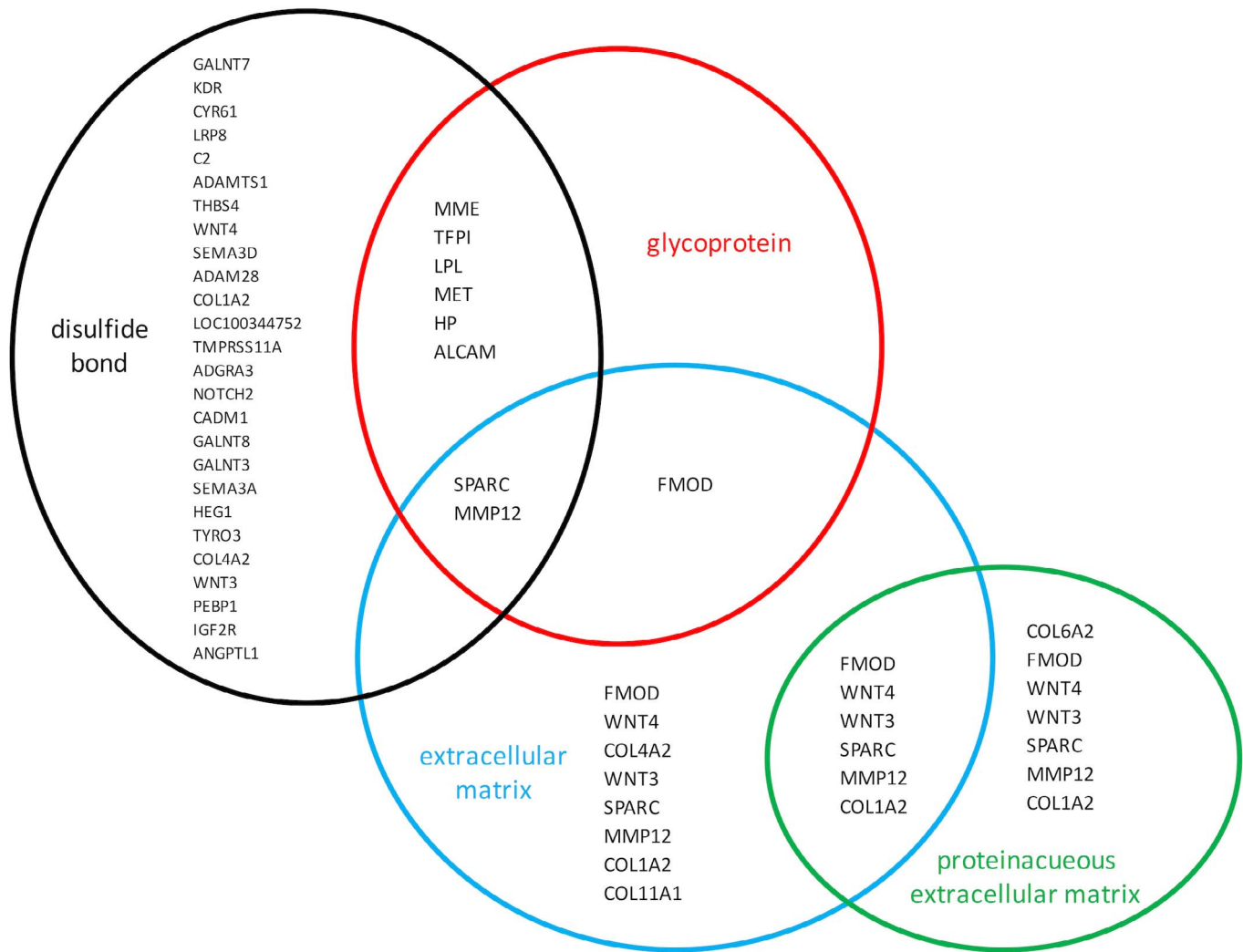


Figure 2. Signaling pathways with specific genes that were significantly affected by CXL treatment and are likely to be involved in corneal stiffness.

remodeling. Among its highest correlated genes were structural extracellular matrix components, including collagen (types I, II, VI, XI), keratocan, and fibromodulin.

Discussion

We analyzed differential gene transcription induced by CXL treatment and observed a significant remodeling of the ECM, including changes in collagen synthesis, glycan biosynthesis, and proteoglycan glycosylation.

Fibrillar collagen types I and XI were downregulated after CXL, while the epithelial basement membrane constituting³⁴ collagen type IV was upregulated. Decreased collagen types I and XI transcrip-

tion potentially results from a reduced collagen degradation after CXL, while increased collagen type IV may be attributed to the recent re-epithelialization and continuing epithelial remodeling.

The activity of enzymes related to glycosylation (enolase 1, transketolase) and, hence, to ECM degradation, was decreased after CXL treatment. Previously, enolase 1 and transketolase overexpression had been reported in context with increased ECM degradation and cancer invasion.^{35–37} Interestingly, a reduced expression of enolase, transketolase, and the protease inhibitor α 2-macroglobulin-like 1 has been reported in keratoconus,^{38–46} which, however, was not able to prevent corneal ectasia.

In contrast, other genes were inversely differentially transcribed after CXL treatment when compared to

Table 2. Genes that Were Significantly Differently Transcribed in a Stiffening-Dependent Manner

Gene	External Name	Chromosome	Description
<i>ENSOCUG00000006901</i>	ANKRD1	18	Ankyrin repeat domain-containing protein 1
<i>ENSOCUG000000011970</i>	TAGLN	1	Transgelin
<i>ENSOCUG000000008236</i>	LPL	15	Lipoprotein lipase-like precursor
<i>ENSOCUG000000026419</i>	DHFR	11	Dihydrofolate Reductase
<i>ENSOCUG000000003636</i>	TGM2	4	Transglutaminase 2
<i>ENSOCUG000000002632</i>	KRT7	4	Keratin 7, type II
<i>ENSOCUG000000012542</i>	CACNA2D3	9	Calcium channel, voltage-dependent, alpha 2/delta subunit 3
<i>ENSOCUG000000014740</i>	SLC37A2	1	Solute carrier family 37 (glucose-6-phosphate transporter), member 2
<i>ENSOCUG000000002272</i>	MYH7B	4	Myosin, heavy chain 7B, cardiac muscle, beta
<i>ENSOCUG000000017128</i>	NMU	15	Neuromedin U
<i>ENSOCUG000000015001</i>	CYB5R2	1	Cytochrome b5 reductase 2
<i>ENSOCUG000000011919</i>	SEMA3A	10	Sema domain, immunoglobulin domain (Ig), short basic domain, secreted, (semaphorin) 3A
<i>ENSOCUG000000000023</i>	PKP2	8	Plakophilin 2
<i>ENSOCUG000000014012</i>	A2ML1	8	Alpha-2-macroglobulin-like 1
<i>ENSOCUG000000006999</i>	C2	12	Complement component 2
<i>ENSOCUG000000003876</i>	FHDC1	15	FH2 domain containing 1
<i>ENSOCUG000000017894</i>	NFKBIE	12	Nuclear factor of kappa light polypeptide gene enhancer in B-cells inhibitor, epsilon
<i>ENSOCUG000000001869</i>	MUC21	12	Mucin 21, cell surface associated
<i>ENSOCUG000000003858</i>	GNMT	12	Glycine N-methyltransferase
<i>ENSOCUG000000029530</i>	CENPH	11	Centromere protein H
<i>ENSOCUG000000027827</i>	CXCL16	19	Chemokine (C-X-C motif) ligand 16
<i>ENSOCUG000000001419</i>	CSAD	4	Cysteine sulfinic acid decarboxylase
<i>ENSOCUG000000005127</i>		11	Uncharacterized protein
<i>ENSOCUG000000014805</i>	WNT3	19	Wingless-type MMTV integration site family, member 3
<i>ENSOCUG000000015904</i>	TKT	9	Transketolase
<i>ENSOCUG000000010331</i>	FAM92A1	3	Family with sequence similarity 92, member A1
<i>ENSOCUG000000003862</i>	DUT	17	Deoxyuridine triphosphatase

keratoconus: collagen type I, keratocan, and thrombospondin 4 were downregulated after CXL, but upregulated in keratoconus.^{41,47} These ECM components potentially may be involved in extracellular remodeling resulting from the increased corneal stiffness after CXL. Thrombospondin 4 has been identified previously as a mechano-sensing molecule in the cardiac contractile response to mechanical stress showing upregulation in response to hypertension.⁴⁸ After CXL-treatment, the mechanical stress resistance

increases and, as a consequence, the tissue strain decreases, which may have led to the downregulation of thrombospondin 4. In the same line, in keratoconus, where increased tissue strain in the cone region is observed, an overexpression of thrombospondin 4 has been reported. Further potential mechano-sensitive genes may be involved in the molecular signaling after CXL treatment (see [Table 2](#)), which in turn could modify the transcription of nonmechano-sensitive genes (see [Supplementary Table S1](#)).

Table 2. Extended

Average Normalized Counts					SD Normalized Counts				
Virgin	Riboflavin	3 mW	9 mW	18 mW	Virgin	Riboflavin	3 mW	9 mW	18 mW
0.00	0.00	10.67	0.6667	0.3333	0.00	0.00	4.51	0.5774	0.5774
0.00	0.00	7.67	1.6667	1.3333	0.00	0.00	1.53	0.5774	0.5774
1.33	1.33	53.33	10.3333	7.6667	0.58	0.58	18.45	14.4684	4.7258
82.33	88.67	0.67	6.3333	14.3333	65.65	73.66	0.58	4.5092	12.5033
17.00	14.33	393.67	104.0000	36.0000	8.54	12.86	151.96	95.3939	28.4781
16.33	21.67	308.33	99.3333	91.6667	7.37	19.14	26.50	9.2376	57.8302
7.67	4.67	0.67	2.0000	2.0000	1.53	2.08	0.58	1.0000	1.0000
5.00	3.33	23.67	9.0000	9.3333	1.00	0.58	15.89	3.0000	1.5275
3.33	4.00	0.33	1.3333	1.6667	1.53	1.00	0.58	0.5774	1.1547
4.67	6.00	0.33	1.6667	3.0000	1.53	3.00	0.58	1.1547	2.6458
91.33	127.33	9.00	32.3333	64.3333	33.98	44.06	2.00	20.5508	19.6044
27.00	36.33	142.00	78.6667	73.6667	7.55	9.87	25.24	19.5533	30.6649
17.00	13.67	77.33	35.3333	27.6667	9.54	5.86	12.10	9.5044	9.0738
393.67	447.00	47.67	170.0000	199.6667	59.00	55.56	7.23	63.8357	109.9288
5.67	5.00	27.33	12.0000	9.0000	2.08	3.46	13.61	3.4641	3.6056
13.33	10.00	46.33	26.6667	23.3333	4.93	1.00	8.39	10.0664	7.7675
9.67	7.67	34.67	16.0000	13.3333	1.53	2.08	6.81	1.0000	4.0415
381.33	322.00	1126.67	680.6667	675.6667	119.78	133.63	174.95	19.2959	38.6566
73.67	111.00	19.67	39.3333	59.6667	24.66	55.22	1.53	19.5533	5.6862
17.00	21.67	5.67	10.0000	10.6667	6.00	3.79	1.53	1.0000	1.5275
14.00	14.00	45.00	23.0000	20.3333	3.00	5.29	5.29	1.7321	1.5275
114.33	118.33	45.33	65.0000	66.3333	16.29	18.45	6.66	8.7178	10.6927
87.67	101.67	35.33	54.6667	56.6667	9.29	14.01	16.04	1.5275	9.2916
91.33	103.00	31.33	59.6667	63.3333	26.63	18.52	3.51	10.2144	20.6478
10,385.67	9981.00	3718.33	6365.3333	7070.0000	1039.99	395.81	361.28	1185.9049	1477.5155
42.00	46.33	17.33	28.0000	34.3333	9.17	11.55	4.16	3.6056	2.0817
27.33	31.00	11.33	17.6667	24.0000	7.51	4.36	3.06	1.1547	4.5826

One of the identified stiffening-independent mechanisms of CXL was the increase in enzymatic proteoglycan glycosylation and glycan biosynthesis (Table 3). β 1,3-galactosyltransferase 2 is involved in the N-acetyl-D-glucosamine sugar addition on the keratan sulfate proteoglycan. A deficiency in a similar enzyme, β 1–4 galactosyltransferase 7, has been associated with Ehlers-Danlos syndrome,⁴⁹ which manifests in joint hyperelasticity and previously also has been reported in context with corneal curvature

abnormalities, including keratoconus, keratoglobus, and cornea plana.^{50,51} These pathologies likely arise from an alteration of corneal stiffness. Other conditions that affect corneal stiffness include diabetes and aging, in which nonenzymatic glycation is increased.^{52,53} In contrast with increased enzymatic glycosylation (as observed after CXL), increased nonenzymatic glycation is a random process that makes it less specific in ECM crosslinking.

Table 2. Extended

log10 (cum_P Value)	Cum_logFC	Remark
8.41	inf	
11.03	inf	Increased expression in keratoconus ⁴¹
6.31	4.16	
7.22	−3.59	
7.53	3.51	Increased expression in vitro after CXL treatment; ⁴³ catalyzes covalent crosslinking e-(g-glutamyl) lysine bonds
8.25	3.13	Increased in keratoconus ⁵⁴
8.29	−1.99	
7.13	1.75	Involved in glycogenolysis and gluconeogenesis; channels excess sugar phosphates to glycolysis in the pentose phosphate pathway
7.03	−1.72	
7.01	−1.68	
9.07	−1.63	
8.83	1.63	
6.18	1.61	
8.95	−1.60	Decreased in keratoconus; ⁴⁵ inhibitor of several proteases
5.83	1.59	
8.64	1.46	
7.63	1.30	
8.70	1.23	
6.10	−1.22	Involved in gluconeogenesis ⁵⁵
7.89	−1.14	
7.64	1.07	
10.51	−0.98	
7.20	−0.95	
7.33	−0.92	
7.40	−0.83	Decreased expression in keratoconus epithelium; ⁴² involved in glycosaminoglycan metabolism; disulfide as acceptor
7.46	−0.73	
7.29	−0.72	

Although the 18 mW/cm² condition was excluded to identify the significantly differentially transcribed genes between crosslinked and control corneas, its expression levels either were in a similar absolute range as the 3 and 9 mW/cm² conditions, or did confirm the gradient between the 3 and 9 mW/cm² conditions. This can be considered as an additional quality control, but at the same time emphasizes the fact that CXL protocols differ on the molecular level in an irradiance/time dependent way.

In absence of an animal model of keratoconus, we used healthy corneas in the experimental groups. It remains to be investigated, if the identified pathways differ in keratoconic corneas. Also, more studies are needed to fully understand the interaction between gene transcription and phenotypic response after CXL. Although it would have been interesting to validate the significantly transcribed genes on the proteomic level, this aspect was out of scope of this study given the high number of

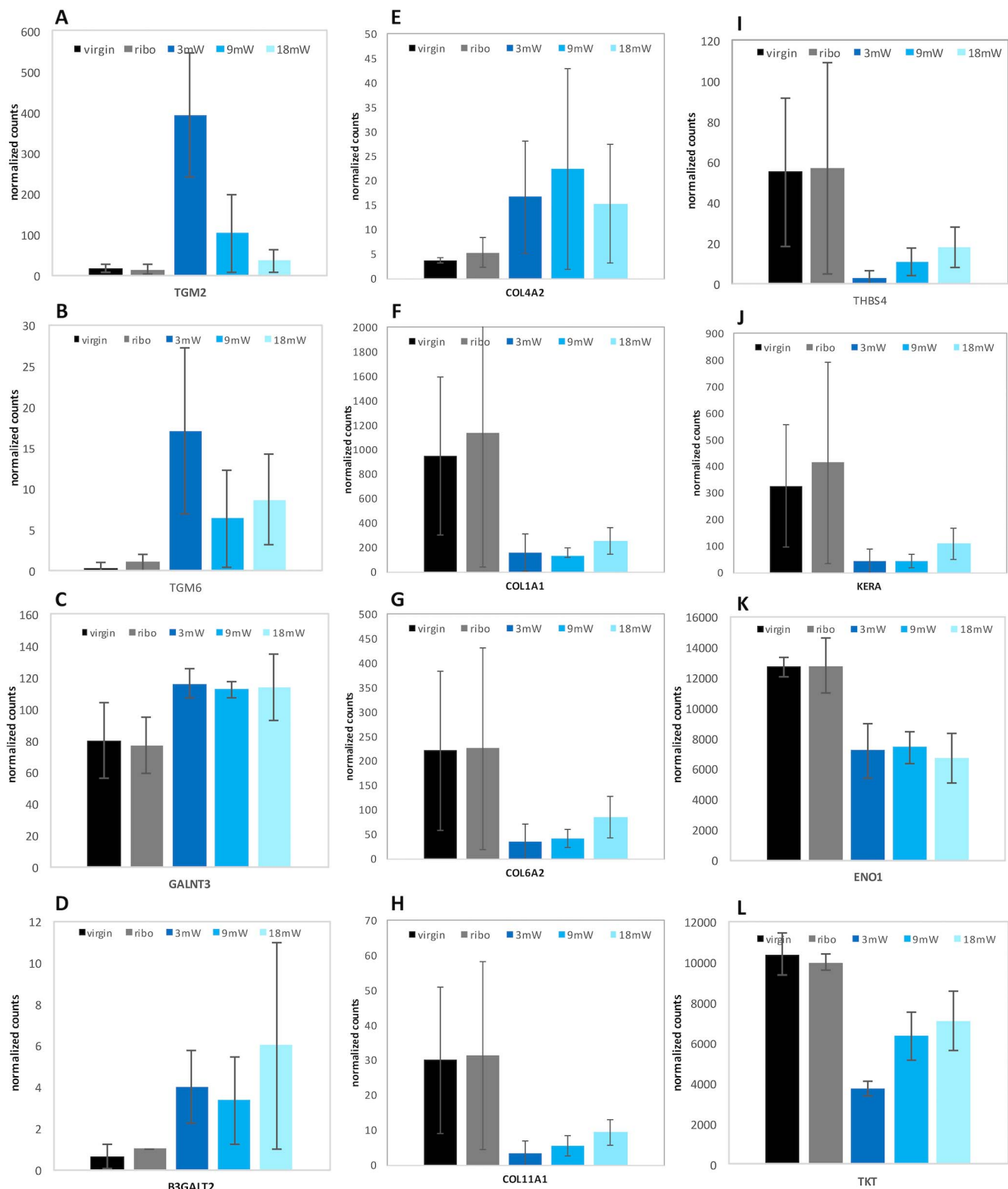


Figure 3. Changes in the normalized counts of transcription for selected genes: (A, B) related to enzymatic crosslinking, (C, D) related to proteoglycan glycosylation, (E–H) structural ECM components, (I, J) other ECM components, and (K, L) related to ECM degradation.

Table 3. Significantly Differentially Transcribed Genes of the Two Strongest Affected Pathways 1 Week After CXL Treatment

Ensembl ID	Gene Name	Gene	Cum_logFC	log10 (cum_P Value)
ECM receptor interaction				
ENSOCUG00000012881	Collagen type I alpha 1 chain	<i>COL1A1</i>	−2.53	2.22
ENSOCUG00000009244	Thrombospondin 4	<i>THBS4</i>	−2.39	3.79
ENSOCUG00000013367	Collagen type XI alpha 1 chain	<i>COL11A1</i>	−2.33	2.9
ENSOCUG00000012264	Collagen type I alpha 2 chain	<i>COL1A2</i>	−2.18	2.23
ENSOCUG00000000409	Collagen type VI alpha 2 chain	<i>COL6A2</i>	−2.06	1.78
ENSOCUG00000017726	Integrin subunit alpha 11	<i>ITGA11</i>	−2.03	11.21
ENSOCUG00000013276	Collagen type IV alpha 2 chain	<i>COL4A2</i>	2.01	2.95
Glycan biosynthesis and metabolism				
ENSOCUG00000005127	Dihydrofolate reductase	<i>DHFR</i>	−3.59	7.22
ENSOCUG00000001596	Beta-1,3-galactosyltransferase 2	<i>B3GALT2</i>	2.42	3.3
ENSOCUG00000009557	Polypeptide N-acetylgalactosaminyltransferase 8	<i>GALNT8</i>	2.29	6.9
ENSOCUG00000009957	Tyrosine aminotransferase	<i>TAT</i>	1.58	3.89
ENSOCUG00000002336	Bone marrow stromal cell antigen 1	<i>BST1</i>	−1.01	8.57
ENSOCUG00000001419	Cysteine sulfinic acid decarboxylase	<i>CSAD</i>	−0.98	10.51
ENSOCUG00000011080	Polypeptide N-acetylgalactosaminyltransferase 7	<i>GALNT7</i>	0.94	3.57
ENSOCUG00000000356	Glucosylceramidase beta	<i>GBA</i>	0.93	5.23
ENSOCUG00000010086	Enolase 1	<i>ENO1</i>	−0.85	5.15
ENSOCUG00000008667	Thymidylate synthetase	<i>TYMS</i>	−0.85	9.52
ENSOCUG00000000006	Inositol polyphosphate-1-phosphatase	<i>INPP1</i>	0.83	5.33
ENSOCUG00000015904	Transketolase	<i>TKT</i>	−0.83	7.4
ENSOCUG00000004762	Synaptojanin 2	<i>SYNJ2</i>	−0.8	5.45
ENSOCUG00000010823	Phosphoribosylformylglycinamide synthase	<i>PFAS</i>	−0.77	3.86
ENSOCUG00000003862	Deoxyuridine triphosphatase	<i>DUT</i>	−0.72	7.29
ENSOCUG00000013372	Ribonucleotide reductase catalytic subunit M1	<i>RRM1</i>	−0.69	9.62
ENSOCUG00000004957	Polypeptide N-acetylgalactosaminyltransferase 3	<i>GALNT3</i>	0.54	2.24
ENSOCUG00000004221	Tyrosinase related protein 1	<i>TYRP1</i>	0.28	7.33
ENSOCUG00000028025	Ethanolamine kinase 2	<i>ETNK2</i>	0.24	4.35

identified genes. A further limitation was that we could not separate the differentially transcribed genes according to their origin (keratocytes, epithelial and endothelial cells). Therefore, the results presented here describe the overall response of ECM relevant differential transcription. Future studies may address the individual contribution of keratocytes and epithelial cells, as well as potential effects on wound healing.

In summary, several target genes potentially related to the biomechanical stability and shape of the cornea were identified. Our findings suggest that corneal stiffening after CXL likely results from a decreased ECM degradation in combination with an increased enzymatic glycosylation, and hence, an altered proteoglycan interaction with collagen fibrils. A proteoglycan-based stiffening after CXL also would be in line with previous findings from x-ray scattering.¹⁸

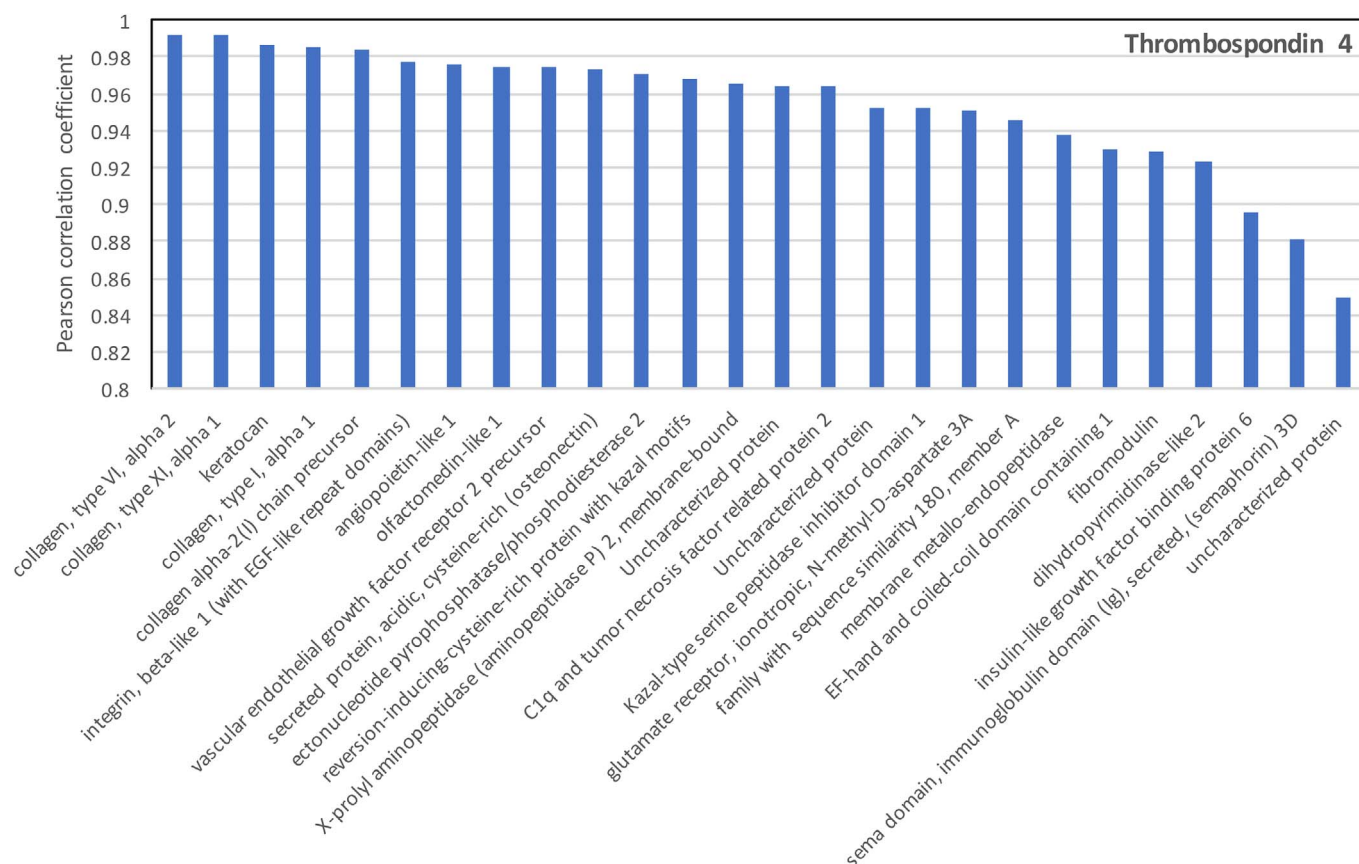


Figure 4. Very strongly correlating ($c_{\text{pearson}} > 0.8$) genes with thrombospondin 4.

Acknowledgements

The authors thank Alain Conti for his skilled technical assistance.

Supported by the Gelbert Foundation (Geneva, Switzerland).

Disclosure: **S. Kling**, None; **A. Hammer**, None; **E. A. Torres Netto**, None; **F. Hafezi**, None

References

1. Spörl E, Huhle M, Kasper M, Seiler T. Increased rigidity of the cornea caused by intrastromal cross-linking [in German]. *Ophthalmologie*. 1997; 94:902–906.
2. Wollensak G, Spörl E, Seiler T. Treatment of keratoconus by collagen cross linking [in German]. *Ophthalmologie*. 2003;100:44–49.
3. Hafezi F, Kanellopoulos J, Wiltfang R, Seiler T. Corneal collagen crosslinking with riboflavin and ultraviolet A to treat induced keratectasia after laser in situ keratomileusis. *J Cataract Refr Surg*. 2007;33:2035–2040.
4. Tomita M, Mita M, Huseynova T. Accelerated versus conventional corneal collagen crosslinking. *J Cataract Refr Surg*. 2014;40:1013–1020.
5. Kymionis GD, Tsoulfaras KI, Grentzelos MA, et al. Corneal stroma demarcation line after standard and high-intensity collagen crosslinking determined with anterior segment optical coherence tomography. *J Cataract Refr Surg*. 2014;40: 736–740.
6. Peyman A, Nouralishahi A, Hafezi F, Kling S, Peyman M. Stromal demarcation line in pulsed versus continuous light accelerated corneal cross-linking for keratoconus. *J Refract Surg*. 2016;32: 206–208.
7. Ng ALK, Chan TC, Cheng AC. Conventional versus accelerated corneal collagen cross-linking in the treatment of keratoconus. *Clin Exp Ophthalmol*. 2016;44:8–14.

8. Hashemi H, Miraftab M, Seyedian MA, et al. Long-term results of an accelerated corneal cross-linking protocol (18 mW/cm²) for the treatment of progressive keratoconus. *Am J Ophthalmol*. 2015;160:1164–1170.
9. Wernli J, Schumacher S, Spoerl E, Mrochen M. The efficacy of corneal cross-linking shows a sudden decrease with very high intensity UV light and short treatment time. *Invest Ophthalmol Vis Sci*. 2013;54:1176–1180.
10. Hammer A, Richoz O, Mosquera SA, Tabibian D, Hoogewoud F, Hafezi F. Corneal biomechanical properties at different corneal cross-linking (CXL) irradiances. *Invest Ophthalmol Vis Sci*. 2014;55:2881–2884.
11. Aldahlawi NH, Hayes S, O'Brart DP, Meek KM. Standard versus accelerated riboflavin-ultraviolet corneal collagen crosslinking: resistance against enzymatic digestion. *J Cataract Refr Surg*. 2015;41:1989–1996.
12. Bikbova G, Bikbov M. Transepithelial corneal collagen cross-linking by iontophoresis of riboflavin. *Acta Ophthalmol*. 2014;92:e30–e34.
13. Leccisotti A, Islam T. Transepithelial corneal collagen crosslinking in keratoconus. *J Refract Surg*. 2010;26:942–948.
14. Hafezi F, Mrochen M, Iseli HP, Seiler T. Collagen crosslinking with ultraviolet-A and hypoosmolar riboflavin solution in thin corneas. *J Cataract Refr Surg*. 2009;35:621–624.
15. Mazzotta C, Traversi C, Caragiuli S, Rechichi M. Pulsed vs continuous light accelerated corneal collagen crosslinking: in vivo qualitative investigation by confocal microscopy and corneal OCT. *Eye*. 2014;28:1179–1183.
16. Jacob S, Kumar DA, Agarwal A, Basu S, Sinha P, Agarwal A. Contact lens-assisted collagen cross-linking (CACXL): a new technique for cross-linking thin corneas. *J Refr Surg*. 2014;30:366.
17. Seiler TG, Fischinger I, Koller T, Zapp D, Frueh BE, Seiler T. Customized corneal cross-linking: one-year results. *Am J Ophthalmol*. 2016;166:14–21.
18. Hayes S, Kamma-Lorger CS, Boote C, et al. The effect of riboflavin/UVA collagen cross-linking therapy on the structure and hydrodynamic behaviour of the ungulate and rabbit corneal stroma. *PloS One*. 2013;8:e52860.
19. Kontadakis GA, Ginis H, Karyotakis N, et al. In vitro effect of corneal collagen cross-linking on corneal hydration properties and stiffness. *Graef Arch Clin Exp*. 2013;251:543–547.
20. Cheng X, Pinsky PM. Mechanisms of self-organization for the collagen fibril lattice in the human cornea. *J R Soc Interface*. 2013;10:20130512.
21. Pinsky PM, Hatami-Marbini H. Modeling collagen-proteoglycan structural interactions in the corneal stroma. *Invest Ophthalmol Vis Sci*. 2011;52:4382–4382.
22. Kanellopoulos AJ. Novel myopic refractive correction with transepithelial very high-fluence collagen cross-linking applied in a customized pattern: early clinical results of a feasibility study. *Clin Ophthalmol*. 2014;8:697.
23. Raiskup-Wolf F, Hoyer A, Spoerl E, Pillunat LE. Collagen crosslinking with riboflavin and ultraviolet-A light in keratoconus: long-term results. *J Cataract Refr Surg*. 2008;34:796–801.
24. Koller T, Pajic B, Vinciguerra P, Seiler T. Flattening of the cornea after collagen cross-linking for keratoconus. *J Cataract Refr Surg*. 2011;37:1488–1492.
25. D'Autréaux B, Toledano MB. ROS as signalling molecules: mechanisms that generate specificity in ROS homeostasis. *Nat Rev Mol Cell Biol*. 2007;8:813–824.
26. Hancock J, Desikan R, Neill S. Role of reactive oxygen species in cell signalling pathways. *Biochem Soc T*. 2001;29:345–349.
27. Hoffman BD, Grashoff C, Schwartz MA. Dynamic molecular processes mediate cellular mechanotransduction. *Nature*. 2011;475:316–323.
28. Wang N, Tytell JD, Ingber DE. Mechanotransduction at a distance: mechanically coupling the extracellular matrix with the nucleus. *Nat Rev Mol Cell Biol*. 2009;10:75–82.
29. Liu Z, Tan JL, Cohen DM, et al. Mechanical tugging force regulates the size of cell-cell junctions. *Proc Natl Acad Sci*. 2010;107:9944–9949.
30. Parsons JT, Horwitz AR, Schwartz MA. Cell adhesion: integrating cytoskeletal dynamics and cellular tension. *Nat Rev Mol Cell Biol*. 2010;11:633–643.
31. Olson EN, Nordheim A. Linking actin dynamics and gene transcription to drive cellular motile functions. *Nat Rev Mol Cell Biol*. 2010;11:353–365.
32. Huang DW, Sherman BT, Lempicki RA. Systematic and integrative analysis of large gene lists using DAVID bioinformatics resources. *Nat Protoc*. 2009;4:44–57.
33. Huang DW, Sherman BT, Lempicki RA. Bioinformatics enrichment tools: paths toward the comprehensive functional analysis of large gene lists. *Nucleic Acids Res*. 2008;37:1–13.

34. Nakayasu K, Tanaka M, Konomi H, Hayashi T. Distribution of types I, II, III, IV and V collagen in normal and keratoconus corneas. *Ophthalmic Res.* 1986;18:1–10.
35. Gao J, Zhao R, Xue Y, et al. Role of enolase-1 in response to hypoxia in breast cancer: exploring the mechanisms of action. *Oncol Rep.* 2013;29:1322–1332.
36. Hsiao K-C, Shih N-Y, Fang H-L, et al. Surface α -enolase promotes extracellular matrix degradation and tumor metastasis and represents a new therapeutic target. *PLoS One.* 2013;8:e69354.
37. Xu IM-J, Lai RK-H, Lin S-H, et al. Transketolase counteracts oxidative stress to drive cancer development. *Proc Natl Acad Sci U S A.* 2016;113:E725–E734.
38. Acera A, Vecino E, Rodríguez-Agirretxe I, et al. Changes in tear protein profile in keratoconus disease. *Eye.* 2011;25:1225–1233.
39. Balasubramanian SA, Wasinger VC, Pye DC, Willcox MD. Preliminary identification of differentially expressed tear proteins in keratoconus. *Mol Vis.* 2013;19:2124–2134.
40. Chwa M, Kenney MC, Khin H, Brown DJ. Altered Type VI Collagen Synthesis by Keratoconus Keratocytes in Vitro. *Biochem Biophys Res Co.* 1996;224:760–764.
41. Feng X, Chaerkady R, Kandasamy K, et al. Proteomic Profiling of Corneal Stroma in Keratoconus Patients. *Invest Ophthalmol Vis Sci.* 2010;51:3477–3477.
42. Joseph R, Srivastava O, Pfister R. Differential epithelial and stromal protein profiles in keratoconus and normal human corneas. *Exp Eye Res.* 2011;92:282–298.
43. Kopsachilis N, Tsaousis KT, Tsinopoulos IT, Kruse FE, Welge-Luessen U. A novel mechanism of UV-A and riboflavin-mediated corneal cross-linking through induction of tissue transglutaminases. *Cornea* 2013;32:1034–1039.
44. Nielsen K, Vorum H, Fagerholm P, et al. Proteome profiling of corneal epithelium and identification of marker proteins for keratoconus, a pilot study. *Exp Eye Res.* 2006;82:201–209.
45. Sawaguchi S, Twining SS, Yue B, et al. Alpha 2-macroglobulin levels in normal human and keratoconus corneas. *Invest Ophthalmol Vis Sci.* 1994;35:4008–4014.
46. Srivastava OP, Chandrasekaran D, Pfister RR. Molecular changes in selected epithelial proteins in human keratoconus corneas compared to normal corneas. *Mol Vis.* 2006;12:1615–1625.
47. Wentz-Hunter K, Cheng EL, Ueda J, Sugar J, Yue B. Keratocan expression is increased in the stroma of keratoconus corneas. *Mol Med.* 2001;7:470.
48. Cingolani OH, Kirk JA, Seo K, et al. Thrombospondin-4 is required for stretch-mediated contractility augmentation in cardiac muscle. *Cir Res.* 2011;109:1410–1414.
49. Freeze HH, Schachter H. Chapter 42: Genetic Disorders of Glycosylation. In: Varki A, Cummings RD, Esko JD, et al., eds. *Essentials of Glycobiology*. 2nd ed. Cold Spring Harbor, NY: Cold Spring Harbor Laboratory Press; 2009.
50. Robertson I. Keratoconus and the Ehlers-Danlos syndrome: a new aspect of keratoconus. *Med J Australia.* 1975;1:571–573.
51. Cameron JA. Corneal abnormalities in Ehlers-Danlos syndrome type VI. *Cornea.* 1993;12:54–59.
52. Malik NS, Moss SJ, Ahmed N, Furth AJ, Wall RS, Meek KM. Ageing of the human corneal stroma: structural and biochemical changes. *BBA-Mol Basis Dis.* 1992;1138:222–228.
53. Wolff SP, Jiang ZY, Hunt JV. Protein glycation and oxidative stress in diabetes mellitus and ageing. *Free Radical Bio Med.* 1991;10:339–352.
54. Nielsen K, Birkenkamp-Demtröder K, Ehlers N, Orntoft TF. Identification of differentially expressed genes in keratoconus epithelium analyzed on microarrays. *Invest Ophthalmol Vis Sci.* 2003;44:2466–2476.
55. Song YH, Shiota M, Kuroiwa K, Naito S, Oda Y. The important role of glycine N-methyltransferase in the carcinogenesis and progression of prostate cancer. *Modern Pathol.* 2011;24:1272.